RESEARCH ARTICLE

Morphogenetic events influencing corneal maturation, development, and transparency: Light and electron microscopic study

Nagwa Ibrahim | Abdalla Hifny | Ruwaida Elhanbaly [ID] | Sara M. M. El-Desoky [ID] |
Wafaa Gaber [ID]

Department of Anatomy and Embryology,
Faculty of Veterinary Medicine, Assiut
University, Assiut, Egypt

Correspondence
Wafaa Gaber, Department of Anatomy and
Embryology, Faculty of Veterinary Medicine,
Assiut University, Assiut 71526, Egypt.
Email: wafaa.anatomy@aun.edu.eg

Review Editor: Paul Verkade

Abstract

The development of the cornea is a fascinating process. Its dual origin involves the differentiation of surface ectoderm cells and the migration of mesenchymal cells of neural crest origin. This research aimed to demonstrate the morphogenesis of the rabbit cornea from fetal to postnatal life using light- and electron microscopy, and immunohistochemical analysis. There were 27 rabbit embryos and nine rabbits used. The rabbit cornea begins its prenatal development on the twelfth day of gestation. The surface ectoderm differentiates into the corneal epithelium on day 13. Intriguingly, telocytes were visible within the epithelium. The secondary stroma develops on the sixteenth day of gestation by differentiation of keratocytes. At the age of 2 weeks, the lamellae of collagenous fibers become highly organized, and the stroma becomes avascular, indicating that the cornea has become transparent. Bowman's membrane appears on day 23 of pregnancy and disappears on day 30. The Descemet's membrane appears at this time and continues to thicken postnatally. The corneal endothelium appears on the twentieth gestational day as double layer of flattened cells and becomes a single layer of cuboidal cells on day 30. The spaces between the endothelial cells resemble craters. VEGF immunohistochemical expression increases over the course of development, reaching its peak in the first week after birth before decreasing in all corneal layers and becoming negative in the stroma. In conclusion, numerous morphogenetic events contribute to corneal maturation and transparency, allowing the cornea to perform its vital functions.

KEYWORDS
cornea, EM, telocytes TCs, transparency, VEGF

Research Highlights

- Using light, scanning, and transmission electron microscopy in addition to immunohistochemical techniques, this research aimed to investigate the embryonic origin and developmental changes of the rabbit cornea during pre- and postnatal life.
- The ultrastructural evidence suggests telocytes play a role in epithelial cell proliferation and differentiation, as well as in the proper arrangement of collagenous fiber lamellae within the stroma, which is essential for corneal transparency.

- By the time the eyelids open, the corneal stroma exhibits negative immunostaining for VEGF, indicating that the stroma has become avascular; this is essential for corneal transparency.

1 | INTRODUCTION

Rabbit eyes share numerous histological and anatomical characteristics with humans and other domestic animals. As such, they have been deemed suitable for ophthalmic surgical evaluation and examination of novel ophthalmic surgical strategies (Gwon, 2008). Understanding the histological development of the eye could aid in identifying the time-sensitive point and effect of tissue differentiation exerted by drug administration in rabbit eyes, which are frequently used in experiments and evaluations of ophthalmic drugs (Kurata et al., 2017). The rabbit corneal model was used to understand and diagnose many diseases like fungal and bacterial keratitis (Pinnock et al., 2017) and to evaluate corneal wound healing, corneal epithelium regeneration (Castro-Combs et al., 2008), and corneal refractive surgery (Zhang et al., 2014). Moreover, corneal model development is used in bioengineering grafting, corneal transplantation, and experimental histopathological studies of anterior chamber structures (Higazy et al., 2020).

The cornea is a glistening, transparent portion of the eyeball's outer fibrous tunic. It serves three primary functions: protection of delicate intraocular structures, light transmission, and light refraction. In fact, the cornea is the primary lens of the eye, accounting for 70%–75% of its refractive power (Hogan et al., 1971; Jakobiec & Ozanics, 1982; Maurice, 1985). The cornea consists of five layers, including corneal epithelium and Bowman's layer, a fibrous meshwork. Approximately 90% of the thickness of the cornea is constituted by the stroma, a collagen-rich central layer, and beneath this is Descemet's membrane, which supports the single layer of corneal endothelium (Hayashi et al., 2002). Corneal differentiation is a fascinating and intricate procedure. Its morphogenesis involves the differentiation of surface ectoderm cells and the migration of neural crest-derived mesenchymal cells (Hay, 1980). The differentiation of surface ectoderm gives rise to corneal epithelium. The neural crest-derived mesenchymal cells differentiate into corneal endothelial cells and keratocytes, the stromal fibroblasts (Lovicu et al., 1999).

Understanding corneal differentiation and the mechanisms that maintain its structure and function is of fundamental scientific and medical importance for corneal disorder prevention, diagnosis, and treatment (Foster & Gilbert, 1992; Robinson et al., 1987). Due to the cornea's unusually large size and accessibility, its tissues are relatively simple to examine and serve as model systems for studying numerous aspects of vertebrate organogenesis (Bard et al., 1988). Researchers have been captivated by the origins, development, and structure of the cornea for over a century, but many questions remain unanswered before we can fully comprehend its biosynthesis and organization. Many researchers are focusing on the histological development of the cornea in numerous animal species, but rabbit corneal data is not yet available. This study aims to evaluate the morphogenesis of the cornea using light, scanning, and transmission electron microscopy as well as immunohistochemical techniques to provide a comprehensive analysis of the development and differentiation of the cornea in the white *New Zealand* rabbit.

2 | MATERIALS AND METHODS

The current study has been approved by The Ethical Committee of The Faculty of Veterinary Medicine, Assiut University, Assiut, Egypt, according to The OIE standards for use of animals in research Under the No. 06/2022/0003.

2.1 | Sample collection

This study used samples collected from 27 *New Zealand* white rabbit fetuses on the following gestational days: 12, 13, 14, 16, 18, 20, 23, 27, and 30 days (three fetuses per age). In addition, nine *New Zealand* white rabbits of both sexes were sacrificed on the first and second weeks as well as the first month of postnatal life (three rabbits per age). At 1 month of age, the eyes of a rabbit are usually completely opened and functionally active. The rabbits were obtained from the Research Farm of the Faculty of Agriculture, Assiut University.

2.2 | Tissue preparation for paraffin embedding

The pregnant rabbits were sacrificed, then their uteri were removed. The embryos were swiftly extracted from the uterus and washed with normal saline. The rabbit embryos were obtained and processed as a whole, while rabbit heads were harvested on days 23, 27, and 30 of the final trimester. Eyeballs were collected during the postnatal ages. The specimens were immediately fixed in 10% neutral buffered formalin. The specimens were dehydrated in ascending concentrations of ethanol, cleared in two changes of xylene, impregnated with soft paraffin, and finally embedded in paraffin wax. Using a Richert Leica RM 2125 Microtome, serial sections of 5 μm thickness were cut and mounted on glass slides. The sections were then stained with Harris hematoxylin and eosin for general histological examination and with Crossmon's trichrome stain to identify collagenous fibers (Bancroft et al., 2013).

2.3 | Semithin sections and transmission electron microscopy (TEM)

Small specimens of the cornea at 23, 30 days of gestation, and 1, 2 weeks as well as 1 month of age postnatally were fixed in a mixture of 2.5% paraformaldehyde and 2.5% glutaraldehyde in 0.1 M

phosphate buffer, pH 7.2, overnight at 4°C. (Karnovsky, 1965). They were washed in the phosphate buffer and then post-fixed in 1% osmium tetroxide in the same buffer for 2 h at room temperature. The samples were then dehydrated in ethanol and embedded in Araldite-Epon mixture. Semithin sections (1 μm in thickness) were cut and stained with Toluidine blue and examined under light microscope. Ultrathin sections were stained with uranyl acetate and lead citrate (Reynolds, 1963) and examined under JOEL 100 II transmission electron microscope.

2.4 | Scanning electron microscopy (SEM)

Small corneal samples at 23, 30 days of gestation, 1 week, and 1 month postnatally were washed in 0.1 M phosphate buffer and fixed in a mixture of 2.5% paraformaldehyde and 5% glutaraldehyde in 0.1 M phosphate buffer, pH 7.2, at 4°C for 24 h. Then, they were post-fixed in 1% osmic acid in 0.1 M sodium phosphate buffer for 2 h at room temperature, washed in 0.1 M phosphate buffer at PH 7.2, and dehydrated in ascending ethanol concentrations, followed by amyl acetate. They were dried using liquid CO_2 at the critical point and mounted on metal stubs. They were sputter-coated with gold palladium, examined and photographed by a JEOL (5400 LV) scanning electron microscope.

2.5 | Digitally colored TEM and SEM images

To increase the visual contrast between multiple structures on the same electron micrograph, we have digitally colored telocytes (TCs), making them more visible to readers. The cells were meticulously hand-colored using Adobe Photoshop Software Version 6.

2.6 | Immunohistochemistry

Paraffin sections of 5 μm thick made from the cornea samples collected at 23, 30 gestational days and 1, 2 weeks of age were dewaxed by xylene, rehydrated by ascending grades of alcohol and rinsed by PBS pH 7.4 (3 times for 5 min). Endogenous peroxidase was suppressed by using hydrogen Peroxide block at room temperature. The sections were thoroughly washed by running tap water for an additional 10 min. To enhance antigen retrieval, the slides were treated with 10 mm sodium citrate buffer (pH 6.0) at temperature reached 95–98 in a water bath for 20 min. The sections were cooled for 20 min at room temperature and subsequently were washed in PBS (pH 7.4, 3 times for 5 min). Block non-specific background staining was performed by using Ultra V block, for 5 min at room temperature. Ultra V block application did not exceed 10 min (to avoid staining artifact). The primary antibody was applied to the sections overnight at 4°C. The used primary antibody was a mouse anti-rabbit antibody against Vascular Endothelial Growth Factor (VEGF) Mouse (MC; MA1-16629 from Thermo Fisher Scientific/Lab Vision) at dilution

(1:200) in the PBS for 1 h at room temperature. Sections were washed using PBS (at pH 7.4, 3 times for 5 min). The biotinylated secondary antibody was applied for 10 min at room temperature. The Biotinylated secondary antibody was Biotinylated goat Anti-Polyvalent, Rabbit anti mouse IgG Thermo Fisher Scientific, The UK. Lab Vision Corporation, ready to use. Sectioned were washed by PBS (pH 7.4, 3 times for 5 min) and subsequently incubated with streptavidin- peroxidase complex. Thermo Fisher Scientific, UK (LabVision corporation; USA) for10 min at room temperature. Visualization of the bound antibodies was performed using 1drop of DAB plus chromogen to 2 ml of DAB plus substrate. The mixture was applied and incubated at room temperature for 5 min. The incubation processes were carried out in a humid chamber. Harris hematoxylin was used as counters stained for 30 s. The sections were dehydrated using ethanol and isopropanol I and II, cleared in xylene and covered by DPX (Abd-Elhafeez & Soliman, 2017; Abdel-Maksoud et al., 2019). The expression of VEGF in the cornea was examined microscopically using OLYMPUS BX51 microscope and the images were taken using OLYMPUS DP72 camera adapted to the microscope. By assessing the intensity of the immunostaining, the staining of the nucleus and/or cytoplasm by the following amount and color of immunostaining: strong (dark brown to black), moderate (brown), mild (light brown) and negative immunostaining (no immunoreactivity) (Abd-Elkareem, 2017).

3 | RESULTS

On the twelfth day of gestation, mesenchymal tissue appears between the lens vesicle and the surface ectoderm (Figure 1a). On the thirteenth day, the primitive corneal epithelium consisting of one to two layers of irregular cells could be observed (Figure 1b). On the fourteenth day, spaces appear in the mesenchyme between the corneal epithelium and the lens (Figure 1c).

On the sixteenth day of gestation, the spaces within the mesenchyme between the corneal epithelium and the lens coalesce to form a cavity that divides the mesenchyme into a thick anterior portion representing the primary stroma of the cornea and a thin posterior portion representing the pupillary membrane; this cavity is the primitive anterior chamber of the eye. The inner corneal stroma contains a greater concentration of mesenchymal cells than the outer region (Figure 1d). At the periphery of the eye ball, the lens contacts the posterior surface of the cornea. At the same level, the secondary stroma of the cornea is formed consisting of keratocytes embedded in loose fibrillar extra cellular matrix. The keratocytes are flat cells with oval, darkly stained basophilic nuclei and cytoplasmic processes. The corneal epithelium still consists of one to two layers. The basal cell layer is cuboidal, whereas the superficial one is flattened (Figure 1e).

On the eighteenth day of gestation, the inner (posterior) region of the corneal stroma is composed of keratocytes, which become more flattened. Under the corneal epithelium, the outer (anterior) portion contains undifferentiated mesenchymal cells (Figure 1f). At this age, collagen fibers appear as scattered fibers throughout the corneal stroma (Figure 2a). On day 20, the corneal epithelium consists of three
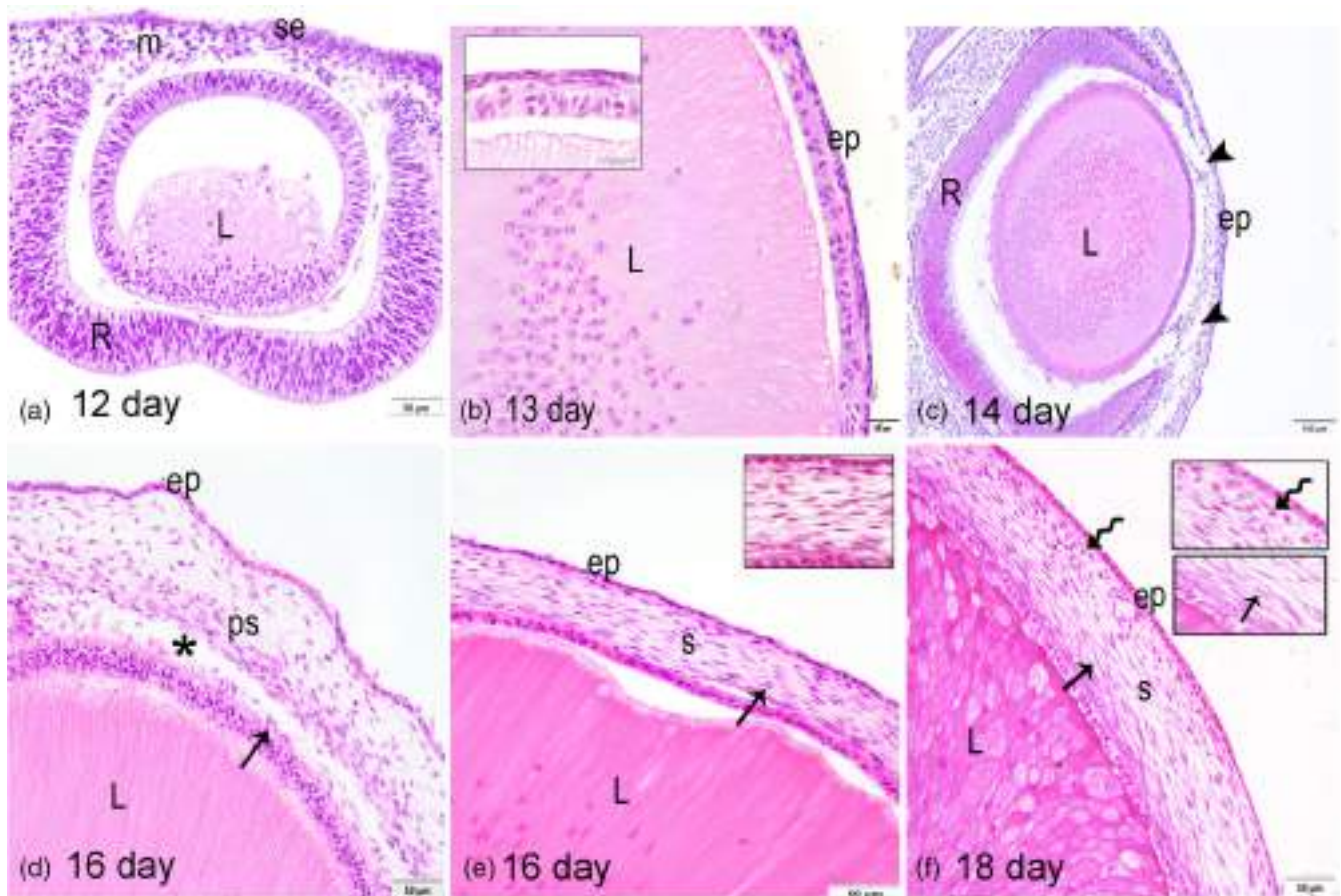
FIGURE 1 Paraffin sections of embryonic rabbit eyes stained with hematoxylin and eosin. (a) On the 12th gestational day shows mesenchyme (m) between the surface ectoderm (se) and the lens (L). Retinal primordium (R). (b) On the 13th gestational day, the corneal epithelium (ep) is formed of one to two layers of irregular cells, inset for higher magnification. (c) On the 14th gestational day shows spaces (arrowheads) in the mesenchymal tissue. (d and e) On the 16th gestational day. (d) The anterior chamber (asterisk) separates the primary stroma (Ps) from the pupillary membrane (arrow). (e) The secondary stroma (s) with characteristic keratocytes (arrow) appears at the periphery of the eye ball, inset for higher magnification. (f) On the 18th gestational day, the differentiated keratocytes (arrow) occupy the inner region of the stroma while the outer part contains mesenchymal cells (zigzag arrow)

to four rows of cells. The basal cells are cuboidal. Superficial to these cells is one to two rows of interdigiting cells, which are covered by flattened epithelial cells (Figure 2b). In the posterior stroma, the collagen fibers are compacted and aligned parallel to one another, whereas in the subepithelial region, there is a small number of interwoven collagen fibers (Figure 2c). At this age, two cell layers of corneal endothelium could be observed lining the anterior chamber (Figure 2d).

With advancement of pregnancy, namely on the 23rd day of gestation, the surface of the corneal epithelium has a polygonal cellular appearance with dark and light cells. On the surface of the cells, microvilli could be observed. They are sporadically distributed over the cell surface and densely arranged along its borders (Figure 3a–c). The corneal epithelium develops four to five rows of cells arranged in three layers: the basal, intermediate, and superficial layers. Undifferentiated cells could be observed between the epithelial cells (Figure 3d). The basal cell layer is composed of two rows of columnar cells. These cells have large euchromatic nuclei and abundant free ribosomes, rough endoplasmic reticulum (RER), and mitochondria in

their cytoplasm (Figure 4a and b). The intermediate layer is formed by polyhedral cells with large euchromatic nuclei. The nuclei occupy the majority of the cell and surrounded by a thin rim of cytoplasm. Telocytes could be observed between the polyhedral cells as ovoid electron dense cell body with variable number of cytoplasmic processes (telopodes). The cell body contains euchromatic nucleus encircled by cytoplasm. The telopodes are thick and short with alternating thin segments (podomers) and dilated cistern-like portions (podoms). It contains secretory vesicles, RER, mitochondria, and caveolae. Moreover, secretory vesicles could be observed in the interstitium between the cells (Figure 4c–f).

Bowman's membrane could be observed as an acellular eosinophilic membrane between the corneal epithelium and secondary stroma (Figure 5a). The density of the corneal stroma's collagen fibers increases (Figure 5b). In the subepithelial region of the corneal stroma, undifferentiated mesenchymal cells with large nuclei and minimal cytoplasm are present. These cells are surrounded by an extracellular matrix consisting of interwoven collagenous fibers

FIGURE 2 (a) Paraffin section of embryonic rabbit eye stained with Crossmon's trichrome on the 18th gestational day shows scattered collagen fibers (arrow) in the corneal stroma (s). (b–d) On the 20th gestational day. (b) Toluidine blue-stained semithin section showing the corneal epithelium (ep) consists of 3 to 4 rows of cells. (c) Paraffin section stained with Crossmon's trichrome shows condensed collagen fibers (arrow) in the posterior stroma and a small number of fibers (arrowhead) in the anterior stroma. (d) Paraffin section stained with hematoxylin and eosin showing the corneal endothelium (en) consisting of two cell layers lining the anterior chamber (asterisk)
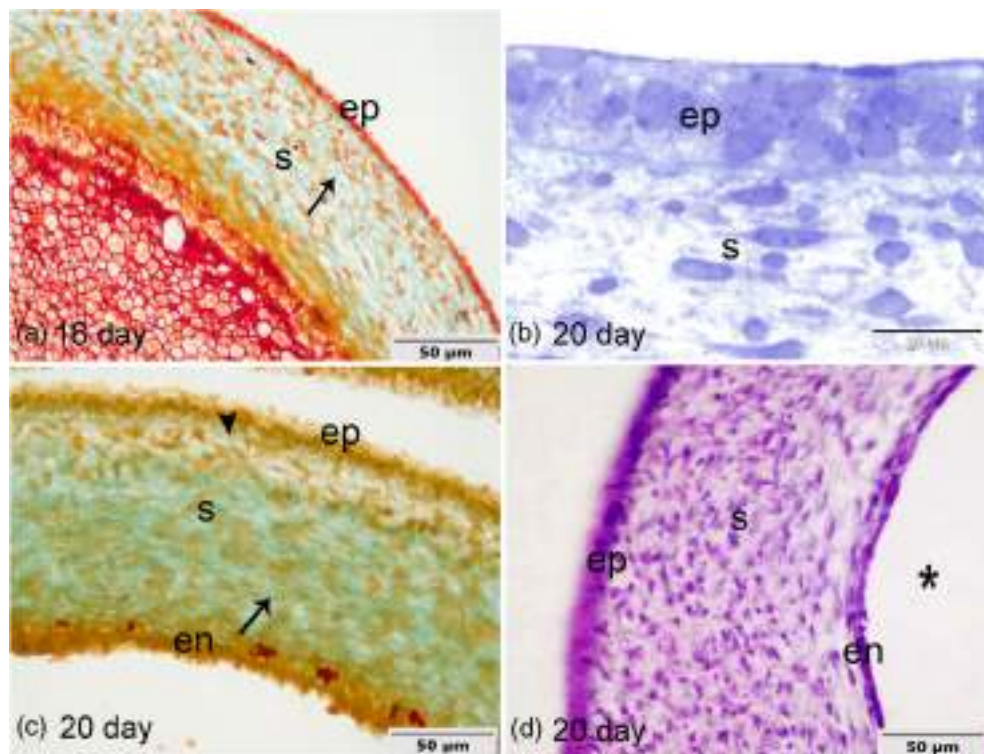

FIGURE 3 (a–c) Scanning electron microscopic (SEM) images showing the surface of the corneal epithelium on the 23rd gestational day. (a) The surface of the corneal epithelium has a polygonal cellular appearance (asterisks). (b) Sporadically distributed microvilli (arrowhead) over the cell surface and densely arranged microvilli (zigzag arrow) along the borders of the cell. (c) Higher magnification showing the surface of the corneal epithelium consists of dark cells (Dc) and light cells (Lc). (d) Toluidine blue-stained semithin section on the 23rd gestational day showing the rabbit corneal epithelium (ep) consists of 4 to 5 rows of cells. Take note of the undifferentiated cells (arrowheads) between the epithelial cells. Stroma (s)
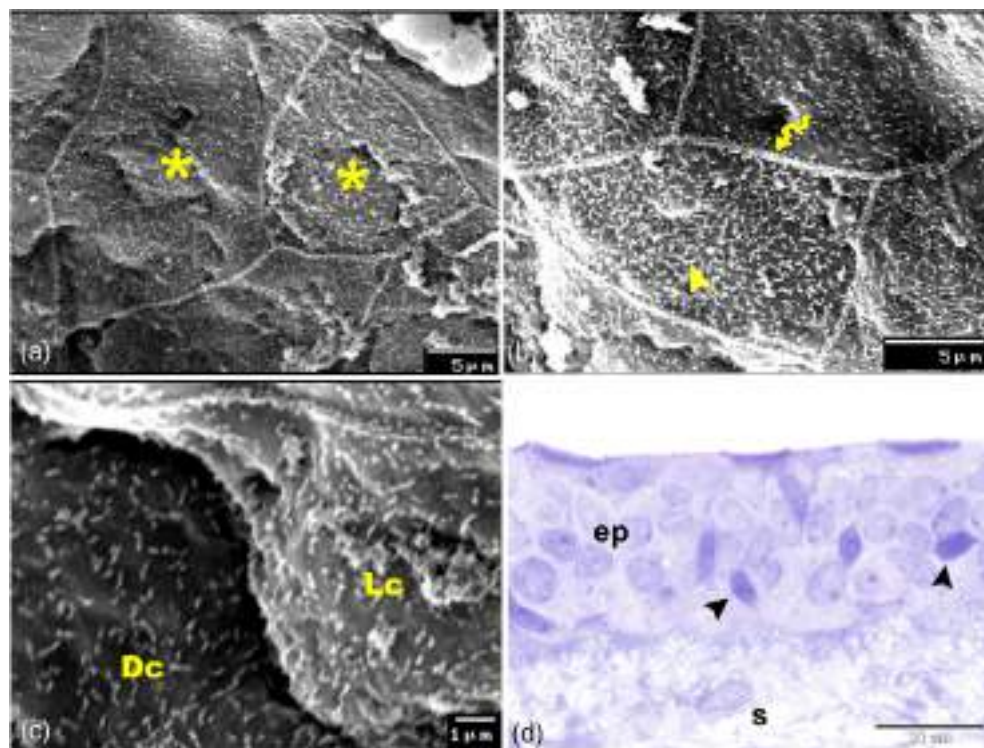
(Figure 5c). In the posterior stroma, collagen fibers are arranged in parallel lamellae interconnected by fine fibrils. The flat connective tissue cells, known as keratocytes, are positioned between the lamellae of collagenous fibers. They have an oval elongated nucleus and cytoplasmic processes. The latter contain RER and mitochondria. In this region, wide spaces between the bundles of collagenous fibers were observed (Figure 5d and e). A single layer of flattened squamous cells comprises the corneal endothelium (Figure 5a). The nuclei of the cells are elongated and euchromatic, and the cytoplasm contains RER and mitochondria (Figure 5f). The internal surface of the corneal endothelium facing the anterior chamber is undulating (Figure 5g).
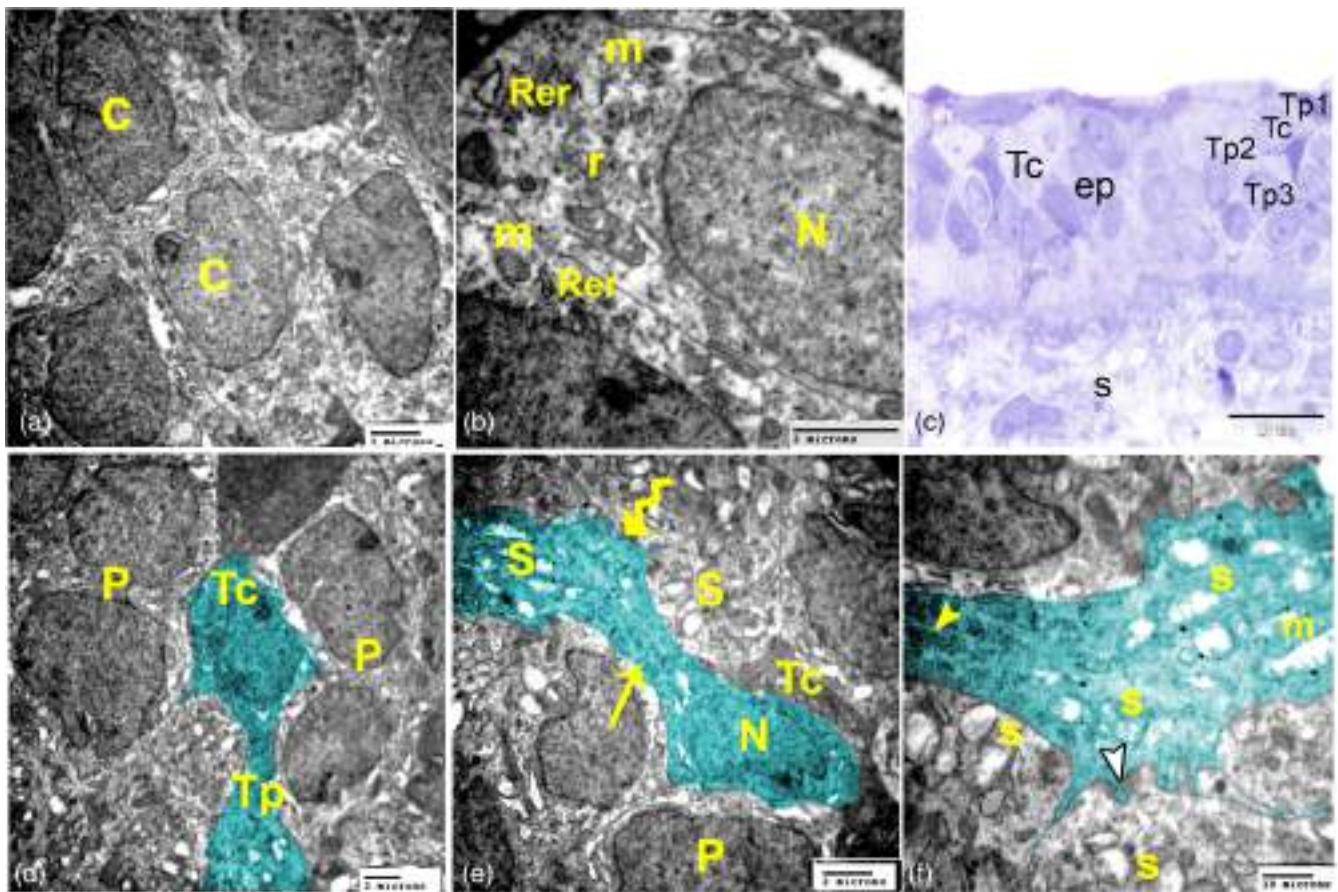
FIGURE 4 (a and b) Transmission electron microscopic (TEM) images of the cornea on the 23rd gestational day displaying the basal columnar cells (c) arranged in two rows and contain nucleus (N), rough endoplasmic reticulum (Rer), mitochondria (m) and free ribosomes (r). (c) Toluidine blue-stained semithin section showing telocytes (Tc) with variable number of telopodes (Tp1, Tp2, Tp3) between the polyhedral cells. d–f: Digitally colored TEM images showing telocytes (Tc, green) between the polyhedral cells (p). podomere (arrow), podom (zigzag arrow), nucleus (N), rough endoplasmic reticulum (arrowhead), mitochondria (m), secretory vesicles (s) and caveolae (white arrowhead). Take note of the secretory vesicles in the interstitium between the cells

On the 27th day of gestation, the corneal epithelium becomes approximately three cells thick, resting on a thick Bowman's membrane (Figure 6a). At the end of gestation, specifically on the thirtieth day of gestation, the microvilli become more numerous. On some cells, they are long and developed, while on others, they are short and poorly developed (Figure 6b). The corneal epithelium is still composed of three layers: the basal layer of columnar cells, the intermediate layer of wing cells, and the superficial layer of flat squamous cells (Figure 6c and d). Through hemidesmosomes, the basal membrane of columnar cells attaches to the basement membrane (Figure 6e). Interdigitations could be observed between the cells of the three layers. A series of desmosomes are observed, ensuring the intercellular junction (Figure 6f). The superficial squamous cells have large flattened oval nuclei and cytoplasm filled with free ribosomes. There are two types of superficial squamous cells, electron-lucent cells with short microplicae on their surface and electron-dense cells with long microvilli (Figure 6g and h).

At this age, Bowman's membrane could not be observed. The corneal stroma continues to be composed of two layers: an anterior fibroareolar layer and a posterior lamellated fibrous layer. The anterior fibroareolar layer is composed of irregularly arranged collagenous fibers and stromal keratocytes arranged in a linear fashion. The posterior lamellated fibrous layer contains relatively dense lamellated collagen fibers and dense stromal keratocytes. Prior to the endothelium, the lamellae are closely spaced and gradually separate as they approach the endothelium (Figure 7a–c). Telocytes could be observed within the corneal stroma connected to the collagen fibers (Figure 7d). The space between the collagen fiber bundles decreases, and keratocytes become flatter and more elongated. In addition to small and large cytoplasmic vesicles, their cytoplasmic processes contain mitochondria, and numerous flattened RER cisternae (Figure 7 e, f).

At this age, the Descemet's membrane appears in underlying the endothelial cells; it could be observed as a continuous layer of a matrix composed of regularly arranged fibrils. On a distinct Descemet's membrane, the cells of the corneal endothelium become cuboidal. Intercellular spaces (gaps) were visible between the endothelial cells, revealing Descemet's membrane layer (Figure 8a and b). The endothelial cells have large euchromatic nucleus. Their cytoplasm
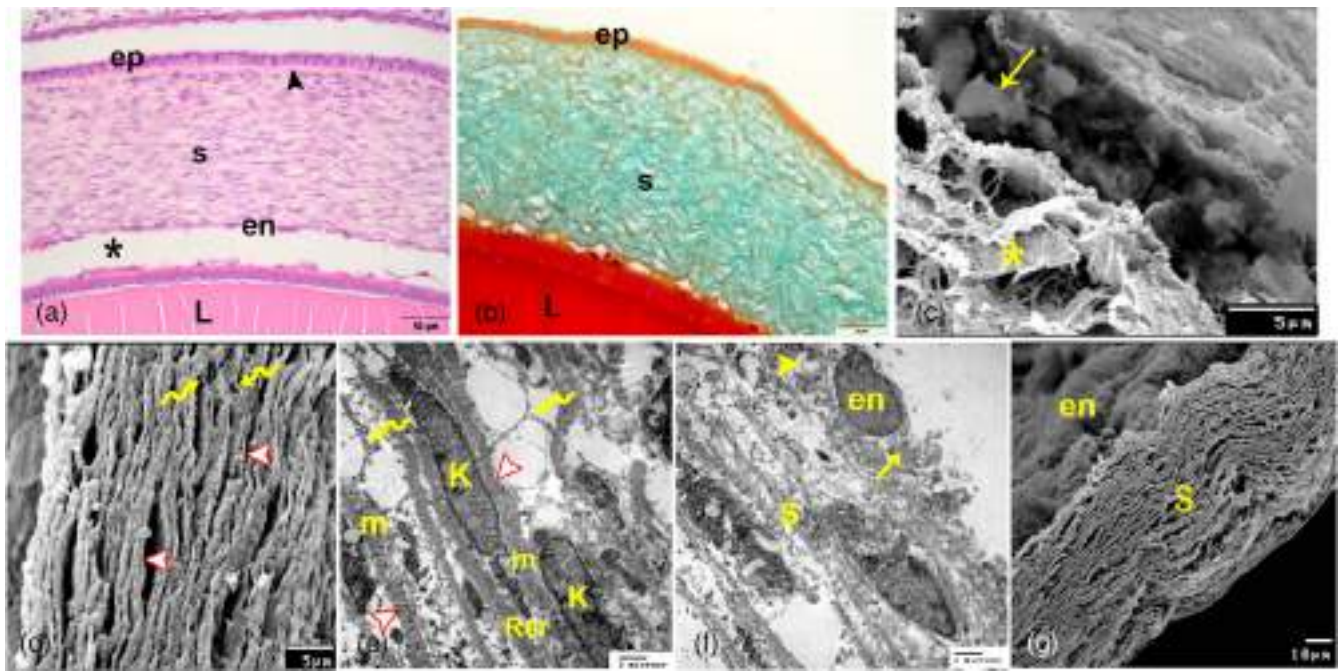
FIGURE 5 Rabbit cornea on the 23rd gestational day. (a) Paraffin section stained with hematoxylin and eosin showing Bowman's membrane (arrowhead) between the epithelium (ep) and the stroma (s). Notice, the corneal endothelium (en) is a single layer of flattened cells lining the anterior chamber (asterisk). Lens (L). (b) Paraffin section stained with Crossmon's trichrome showing abundant of collagen fibers constitute the stroma (s). (c) SEM image show the stroma in the sub epithelial region contains mesenchymal cells (arrow) and intermingled collagen fibers (asterisk). (d and e) are SEM and TEM images respectively show the lamellae of collagenous fibers in the posterior stroma (white arrowheads) are parallel to each other and connected by fine fibrils (zigzag arrows). Take note of the keratocytes between the lamellae (k) with its elongated nucleus, mitochondria (m), and rough endoplasmic reticulum (Rer). f: TEM image shows the endothelial cells (en) contain rough endoplasmic reticulum (arrow) and mitochondria (arrowhead). g: SEM image showing the internal surface of the corneal endothelium (en) is undulating. Stroma (s)

contains abundant of RER, mitochondria and free ribosomes in addition to cytoplasmic vesicles. Solitary cilium could be noted extending from the basal body in the apical cytoplasm of the endothelial cells and protruding into the anterior chamber. A single centriole was observed in vicinity of the basal body of the solitary cilium (Figure 8c). Variable-sized spaces were observed between the basement membranes of adjacent endothelial cells (Figure 8d).

The scanning electron microscope revealed three types of superficial corneal epithelial cells in one-week-old rabbits: light, intermediate, and dark cells. The dark cells' nuclei were distinguishable from the surface. It occupies an eccentric position (Figure 9a). Numerous microvilli cover the apical surface of the cells, giving them a velvety appearance (Figure 9b). The histological structure of the corneal epithelium resembles that of 30-day-old embryos, and the basement membrane is clearly defined (Figure 9c and d). Some basal columnar cells have nuclei that are indented and heterochromatic (Figure 9e). Telocytes could be observed between the basal columnar cells extending their processes to contact with the basement membrane. The cytoplasm of telocytes contains fewer organelles, and no secretory vesicles were detected in the interstitium between the cells (Figure 9f).

At this age, the stroma becomes completely lamellated, consisting of thick, dense and closely arranged lamellae of collagenous fibers interspersed with flattened electron-dense keratocytes in between.

As they approach the endothelium, these lamellae separate from one another (Figure 10a–d). Under a scanning electron microscope, the spaces between the endothelial cells appeared as crater-like structures with elevated borders, revealing the underlying Descemet's membrane (Figure 10e). The cuboidal cells of the corneal endothelium rest on a thick Descemet's membrane. These cells have euchromatic nucleus and cytoplasm rich in RER, mitochondria, rough endoplasmic reticulum-mitochondrial complex, and free ribosomes (Figure 10f).

The corneal epithelium of two-week-old rabbits increases in thickness to become from five to seven cells. The basal and intermediate layers appear to be more densely populated (Figure 10g). The corneal stroma is composed of highly organized lamellae of collagenous fibers that resemble a homogeneous extracellular matrix in which the keratocytes are embedded. The density of these keratocytes gradually decreases as they approach the corneal endothelium, where there are few keratocytes. The spaces between endothelial cells decrease (Figure 10h).

In the one-month-old rabbits, the cornea reaches its adult form. The corneal epithelium is stratified squamous epithelium composed of five to seven cells deep, which rests on a distinct basement membrane. The epithelium's basal cell layer is composed of one row of high- and low-columnar cells with oval nuclei located at the apex. The intermediate layer contains multiple rows of polyhedral cells with a
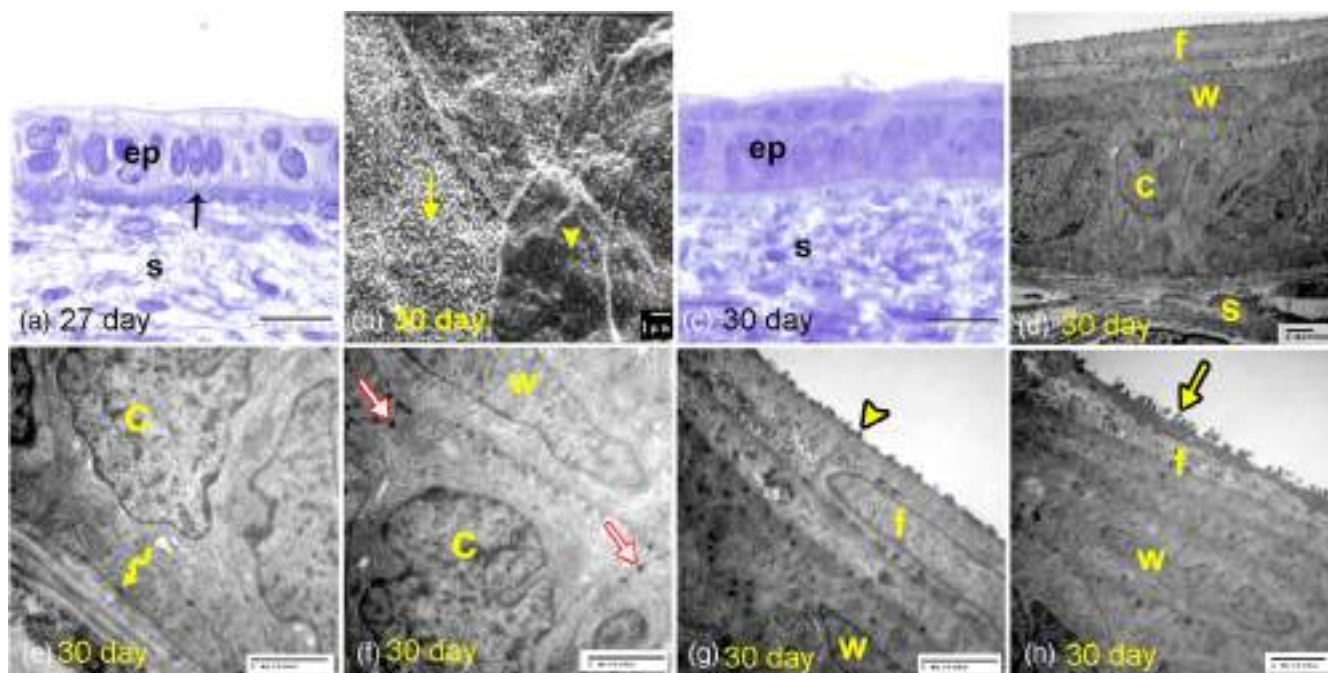
FIGURE 6 (a) Toluidine blue-stained semithin section on the 27th gestational day shows the corneal epithelium (ep) is about 3 cells thick resting on a thick Bowman's membrane (arrow). Stroma (s). (b–h) Corneal epithelium on the 30th gestational day. (b) SEM image showing the microvilli on the surface of the epithelial cells are long well developed (arrow) on some cells and short poorly developed (arrowhead) on others. (c) Semithin section showing 3 cell rows of the corneal epithelium (ep). Stroma (s). (d–h) TEM images showing the corneal epithelium consists of basal layer of columnar cells (c), intermediate layer of wing cells (w) and superficial layer of flat squamous cells (f). Take note of the hemidesmisomes (zigzag arrow) between the basal membrane of the columnar cells and the basement membrane, the series of desmosomes (white arrows) along the interdigitations between the cells, short microplicae (arrowhead) and long microvilli (arrow)

rounded, central nucleus. Furthermore, the superficial layer consists of two to three rows of overlapping squamous cells covered with densely packed microvilli (Figure 11). The collagenous fibers' lamellae have a wavy appearance (Figure 12a–c). The Descemet's membrane is a thick, acellular layer that separates the corneal stroma from the endothelium (Figure 12d), and the gaps between endothelial cells decrease (Figure 12e).

In the developing rabbit cornea, VEGF immunohistochemical expression varied greatly from one developmental stage to the next, reaching its maximum immunopositivity at the end of the first week after birth, after which it decreases in all layers of the cornea.

The immunohistochemical localization of VEGF in the rabbit cornea on the 23rd day of gestation revealed moderate immunostaining in both the corneal epithelium and endothelium. The corneal stroma exhibited mild VEGF immunostaining (Figure 13a–c). Toward the end of gestation, specifically on the thirtieth gestational day, the intensity of VEGF immunoreactive signals increases relative to the preceding phase of development. It is moderate to strong in the corneal epithelium and endothelium, and moderate throughout the corneal stroma (Figure 13d–f).

By the end of the first week after birth, the intensity of VEGF immunoreactive signals in various layers of the rabbit cornea reaches its maximum level (Figure 14a). During the second postnatal week, the immunohistochemical localization of VEGF in the rabbit cornea decreased, and corneal epithelium cells expressed moderate to weak VEGF immunoreactivity. The corneal stroma shows negative immunostaining to VEGF, whereas the keratocytes within the corneal stroma exhibit weak immunostaining. The corneal endothelium exhibited weak VEGF immunoreactivity (Figure 14b–d).

4 | DISCUSSION

On the 12th day of gestation, mesenchymal tissue appears between the surface ectoderm and lens vesicle, marking the beginning of the development of the rabbit cornea. This mesenchyme appears after the lens vesicle, and the surface ectoderm have completely separated, allowing the surrounding mesenchyme to invade and position itself between them. On day 13, the surface ectoderm differentiates into the corneal epithelium, as the infolding of the surface ectoderm to form the eyelids started.

According to our findings, the corneal epithelium attains its adult form 2 weeks postnatally (around the time of the eyelid opening). This is consistent with the findings of (Yamagiwa et al., 2021) for the same species. In addition, Abdo et al. (2017) observed that the corneal epithelium attains full adult morphology at 9 days postnatal. In humans, the corneal epithelium matures at approximately 24 gestational weeks, around the same time that the eyelids open prenatally (Graw, 2003). Therefore, most of the histological maturation of the human corneal epithelium occurs during gestation (Van Cruchten
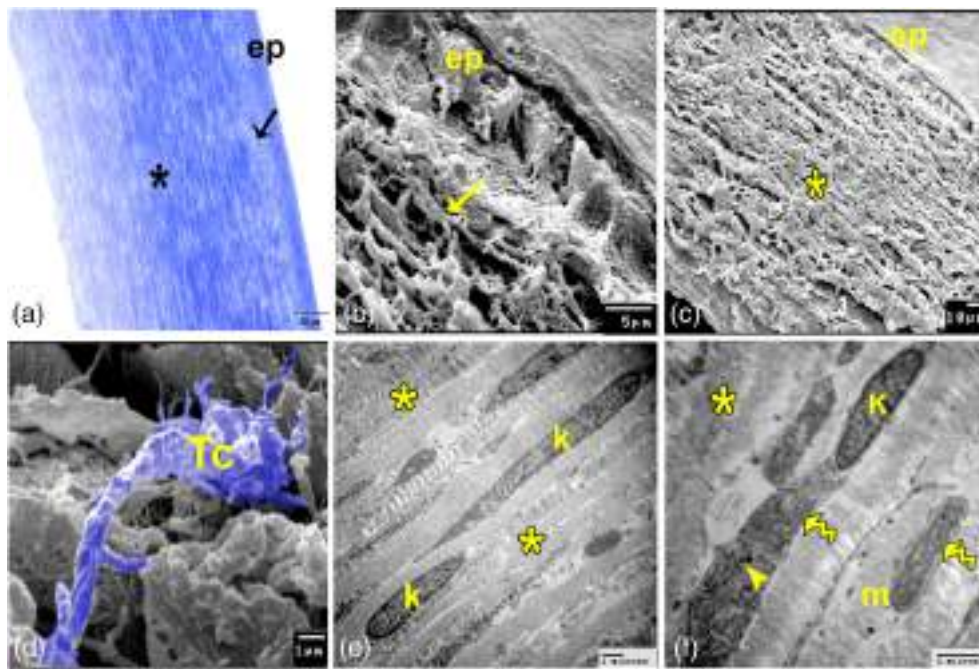
FIGURE 7 Corneal stroma on the 30th gestational day. (a) Semithin section showing the two layers of the corneal stroma; fibroareolar layer (arrow) and posterior lamellated layer (asterisk). Epithelium (ep). (b and c) SEM images showing intermingled collagen fibers (arrow) in the fibroareolar layer and parallel lamellae of collagenous fibers (asterisk) in the posterior lamellated layer of the stroma. (d) A digitally colored SEM image displaying telocyte (Tc, blue) within the corneal stroma. (e and f) TEM images of the stroma showing the lamellae of the collagenous fibers (asterisks) and keratocytes (k). Notice, the cytoplasmic processes of keratocytes contain rough endoplasmic reticulum (zigzag arrows), mitochondria (m) as well as small and large cytoplasmic vesicles (arrowhead)

FIGURE 8 Corneal endothelium on the 30th gestational day. (a) Paraffin section stained with Crossmon's trichrome showing the endothelial cells (en) become cuboidal and there are spaces (arrowheads) between them. Epithelium (ep) and stroma (s). (b–d) TEM images showing the Descemet's membrane (D) between the cuboidal endothelial cells (en) and the stroma (s). Intercellular spaces (asterisks), nucleus (N), rough endoplasmic reticulum (Rer), mitochondria (m), free ribosomes (r), cytoplasmic vesicles (white arrowheads), centriole (c) and solitary cilium (zigzag arrow). Take note of the spaces of varying sizes (arrowheads) between the basement membranes of adjacent endothelial cells
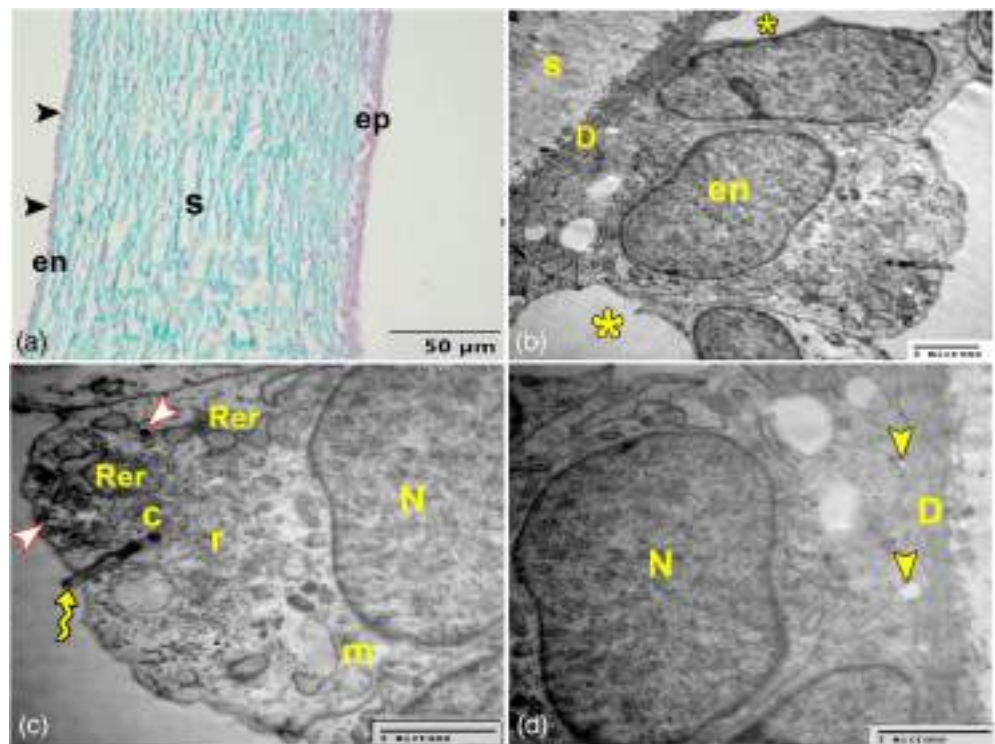
et al., 2017). In rabbits, our results and those of Yamagiwa et al. (2021) confirmed that the epithelium continues to develop histologically after birth. This explains why rabbits are born with their eyes closed. The structures are not fully developed at birth, and the eyelids are separated when they become fully developed and begin to function (El-Desoky & Abdellah, 2022).
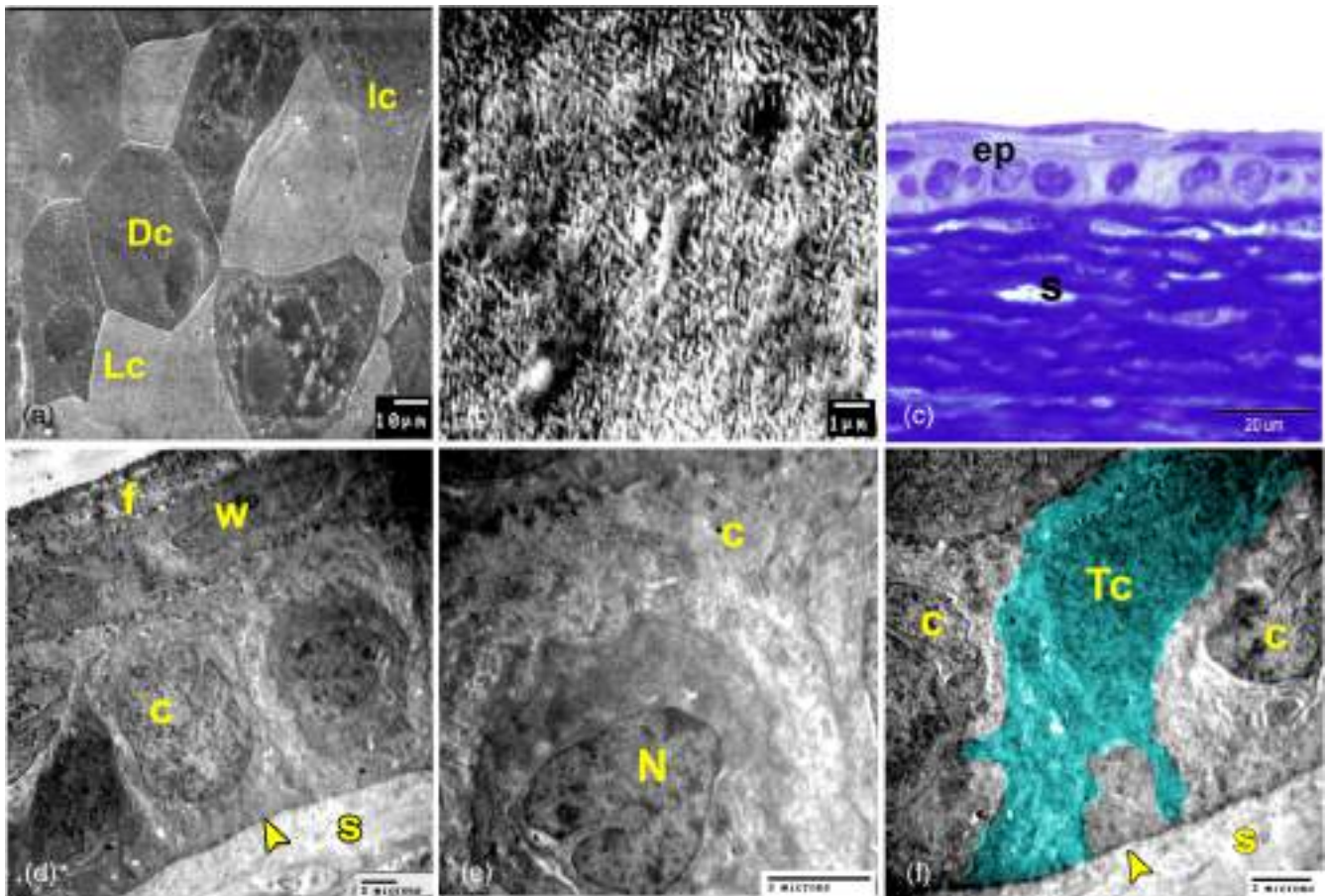
FIGURE 9 Developing cornea of 1 week old rabbit. a and b: SEM images for the surface of the corneal epithelium. (a) Three types of superficial cells; dark cells (Dc), light cells (Lc) and intermediate cells (Ic). (b) The apical surface of the cells is studded by numerous microvilli. (c) Toluidine blue-stained semithin section shows the layers of the epithelium (ep) and the stroma (s). (d and e) TEM images for the corneal epithelium. (d) shows the basal columnar cells (c) resting on distinct basement membrane (arrowhead), intermediate wing cells (w) and superficial flattened cells (f). (e) High magnification shows some basal columnar cells have indented heterochromatic nucleus (N). (f) A digitally colored TEM image displaying telocyte (Tc, green) between the basal columnar cells (c) extending its processes to contact with the basement membrane (arrowhead). Notice, no secretory vesicles present in the interstitium between the cells

The surface of the corneal epithelium has a polygonal cellular appearance and is covered with microvilli, according to SEM findings. The primary function of microvilli is to increase the plasma membrane's surface area, allowing more mucin to be adsorbed and enhancing the tear film's stability (Pfister, 1973). During prenatal development, the surface of the corneal epithelium is composed of dark and light cells. In contrast, it is composed of dark, medium, and light cells during postnatal development. This simulates the mouse model described by Hazlett et al. (1980). The various cell types are transitional stages of the same cell, with light cells being younger than dark cells (Hoffmann, 1972). The dark cell may be dark due to the density or length of the microvilli, the nature of the plasma membrane, the presence of more adsorbed mucin, or a combination of factors, according to Pfister (1973). The light cell could be bright due to inverted factors.

Intriguingly, we observed telocytes (TCs) in the epithelium of the rabbit cornea. Recent studies have described the presence of TCs in the limbus, sclera, and uvea of the mouse (Luesma et al., 2013), in the

corneal stroma of humans (Marini et al., 2017), and in the lung epithelium (Hussein & Mokhtar, 2018; Tang et al., 2022) but not in the corneal epithelium of rabbits. Between the polyhedral cells of the corneal epithelium on the 23rd day of gestation, TCs were visible. Their short telopodes contain RER, mitochondria, and an abundance of secretory vesicles. In the interstitium, the secretory vesicles are shed. This is consistent with Hussein and Mokhtar's (2018) findings that fetal TCs are characterized by short telopodes. Through the release of extracellular vesicles such as exosomes, ectosomes, and multivesicular cargoes, TCs participate in intercellular signaling (Albulescu et al., 2015; Cretoiu et al., 2016). The shed vesicles are essential for stem cell maintenance, vascular hemostasis, immune surveillance, tissue repair, and the release of lipids, proteins, and nucleic acids to meet the target tissue requirements (Cretoiu et al., 2016; Edelstein & Smythies, 2014). The presence of TCs in the epithelium indicates a role in cell proliferation and differentiation (Tang et al., 2022). By the end of gestation, TCs are located between the basal columnar cells and become organelle-deficient and less active.
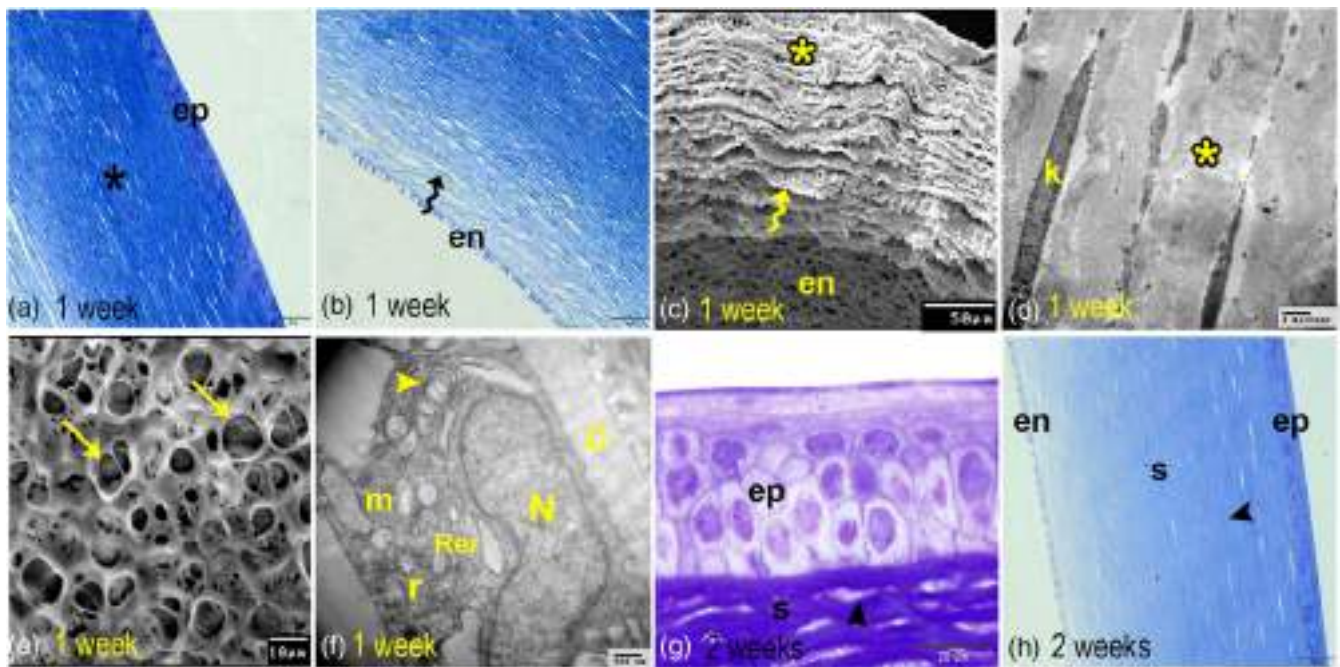
FIGURE 10 Developing cornea of 1 week (a–f) and 2 weeks (g and h) old rabbits. (a and b) Toluidine blue-stained semithin sections, (c) SEM and (d) TEM images showing the corneal stroma consists of thick lamellae of collagenous fibers (asterisk) with keratocytes (k) in between. Notice, the lamellae are separated from each other (zigzag arrow) toward the endothelium (en). (e) SEM image for the surface of the corneal endothelium showing crater like structures with elevated borders (arrows) that represent the spaces between the endothelial cells, revealing the underling Descemet's membrane. (f) TEM image for the endothelial cells resting on a thick Descemet's membrane (D). Nucleus (N), mitochondria (m), rough endoplasmic reticulum (Rer), rough endoplasmic reticulum-mitochondrial complex (arrowhead) and free ribosomes (r). (g and h) Toluidine blue-stained semithin sections showing the corneal epithelium (ep) is 5 to 7 cells thick. Notice, the stroma (s) appears as homogenous extracellular matrix where the keratocytes (arrowhead) are embedded and the spaces between the endothelial cells (en) decrease

The present study revealed that Bowman's membrane appears prenatally on the 23rd day of gestation, which is consistent with previous rabbit studies (Abdo et al., 2017; Hayashi et al., 2002). The Bowman's membrane is a longitudinal condensation formed by the processes of mesenchymal cells in the corneal stroma (Sevel & Isaacs, 1988). On the thirtieth gestational day, we discovered that it had disappeared. This confirms that the cornea of an adult rabbit lacks Bowman's layer, a conclusion supported by the absence of this layer (Cintron et al., 1983).

On the twelfth day of gestation, mesenchymal tissue invades the space between the lens vesicle and the surface ectoderm, initiating the development of the corneal stroma. The detached lens vesicle has a compressive effect on the growth and proliferation of the precursors of the corneal stroma, the mesenchymal cells (Sevel & Isaacs, 1988). On the sixteenth day, the secondary stroma begins to develop with the appearance of keratocytes at the eyeball's periphery. These keratocytes are differentiated from the neural crest cells that have invaded. The migration of neural crest cells results in the formation of stromal keratocytes and corneal endothelium (Haustein, 1983; Pei & Rhodin, 1970; Swamynathan, 2013). On the eighteenth day of gestation, the keratocytes extend centrally to cover the entire length of the cornea, but the anterior portion of the stroma still contains undifferentiated mesenchymal cells. Rapid keratocyte growth is caused by continuous neural crest cell invasion and/or keratocyte

proliferation (Saika et al., 2001). Keratocytes are responsible for producing the highly specialized extracellular matrix (collagenous fibers) of the corneal stroma (Haustein, 1983). On the eighteenth day, keratocytes become more differentiated and begin producing collagenous fibers that appear as scattered fibers throughout the stroma, according to our findings. Mitochondria, numerous RER cisternae, and small and large cytoplasmic vesicles are present in keratocytes to support their secretory role.

According to the present findings, the arrangement of collagen fibers begins on the twentieth day of gestation and extends from posterior to anterior. This replicated Quantock and Young's (2008) in humans. According to this study, the anterior stroma develops later than its posterior counterpart. At the end of gestation, the corneal stroma comprises two layers: the anterior fibroareolar layer and the posterior lamellated fibrous layer. These results are consistent with the findings of Al-Taey and Al-Haaik (2022) in one-day-old rabbits. We demonstrated that corneal stroma development is completed postnatally. Prior to the opening of the eyelids, the entire stroma is a lamellated fibrous layer as the disorganized collagenous fibers of a one-week-old rabbit arrange themselves in the form of parallel lamellae.

After the eyelids of a two-week-old rabbit have opened, the corneal stroma becomes highly organized lamellae of collagenous fibers. This configuration of collagen fibers in the corneal stroma is crucial to
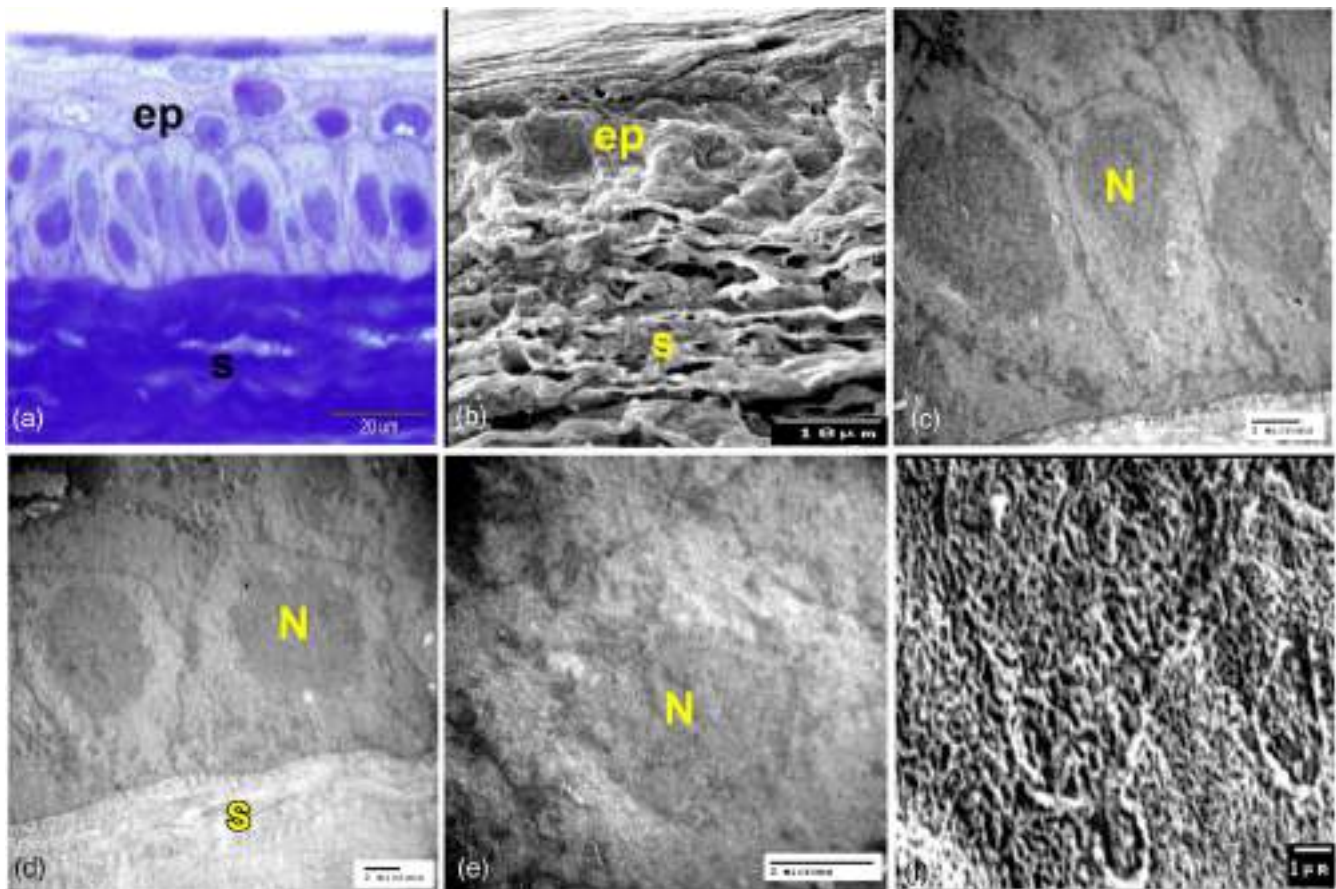
FIGURE 11 Corneal epithelium of 1 month old rabbit. (a) Semithin section and (b) SEM image showing stratified squamous epithelium (ep) and stroma (s) of the cornea. (c–e) TEM images for the corneal epithelium showing (c) The basal high columnar and (d) The basal low columnar cells have oval apical situated nucleus (N). (e) The intermediate polyhedral cells have rounded central nucleus. (f) SEM image showing the apical surface of the cornea is studded with densely packed microvilli

corneal transparency (Harper et al., 2005; Hassell & Birk, 2010). The main functions of the corneal stroma are light protection, transmission, and refraction. These functions are associated with the stroma's highly organized extracellular matrix (Hogan et al., 1971). At 1 month of age, this study revealed that the lamellae of collagenous fibers have a wavy appearance. It is hypothesized that the appearance of waves is due to an increase in lamellae length.

Under a scanning electron microscope, TCs were observed communicating with collagen fibers within the corneal stroma. The uniform distribution of TCs throughout the stroma contributes to the correct assembly and maintenance of a highly organized collagenous matrix, which is necessary for corneal transparency. The reduction and loss of TCs may alter the organization of the extracellular matrix, leading to corneal dysfunctions, as in keratonic cornea (Keratoconus), which is characterized by a severe reduction of TCs in the anterior stroma, with the remaining TCs exhibiting degenerative features (Marini et al., 2017). Progressive corneal protrusion and thinning characterize keratoconus, resulting in irregular astigmatism and impaired visual function. The condition's etiology and pathogenesis are not fully understood, but genetic and environmental factors may be involved (Vazirani & Basu, 2013).

The results of Descemet's membrane (DM) indicated that this layer first appears on the thirtieth day of gestation (end of gestation). It appears as a continuous layer of a fibril-based matrix beneath the endothelial cells. It develops from the processes of the deep mesenchymal cells of the stroma, according to Sevel and Isaacs (1988). However, according to Graw (2003), DM is produced by the corneal endothelium. In this study, the DM developed later than Bowman's membrane (BM), which formed on the 23rd day of gestation. In contrast, Sevel and Isaacs (1988) assert that the DM comes before the BM. Additionally, we discovered that the appearance of DM coincided with the disappearance of BM. According to Merindano et al. (2003), the large thickness of the DM compensates for the absence of the BM in camels. Postnatally, after the opening of the eyelids, the DM continues to thicken (Yamagiwa et al., 2021).

This study shows that the corneal endothelium appears on the twentieth day of gestation. At this age, the anterior chamber's extension from central to peripheral is complete. The corneal endothelium is consequently formed to line the anterior chamber. After keratocyte differentiation, the mesenchymal cells differentiate into endothelial cells. This contradicts Arey's (1965) study on human and Hay's (1980) study on avian. They indicated that mesenchymal cells differentiate
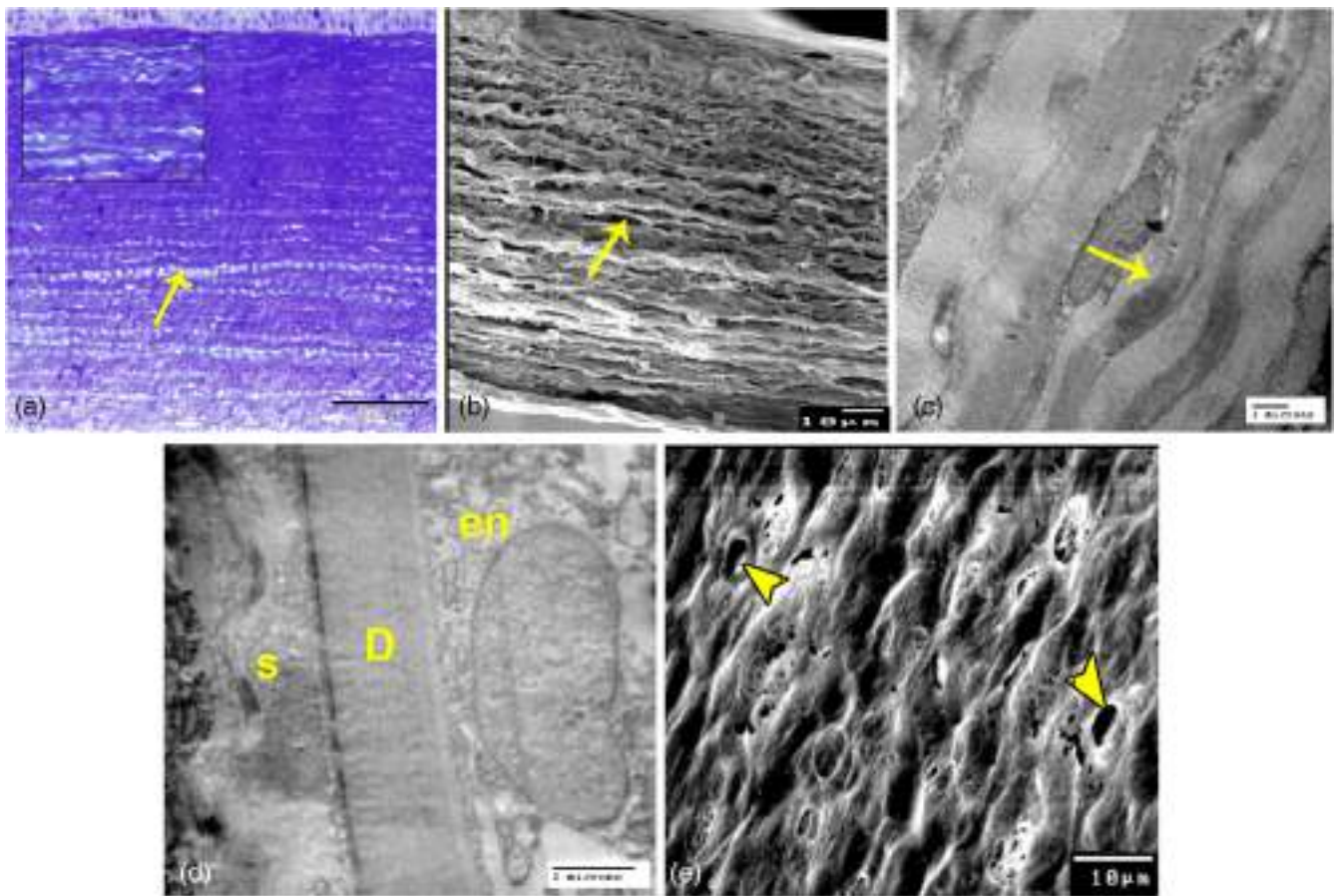
FIGURE 12 Corneal stroma and endothelium of 1 month old rabbit. (a) Toluidine blue-stained semithin section, (b) SEM and (c) TEM images for the corneal stroma showing the lamellae of the collagenous fibers (arrow) have a wavy appearance. (d) TEM image showing very thick Descemet's membrane (D) separates the corneal stroma (s) from the endothelium (en). (e) SEM image showing few narrow gaps (arrowheads) between the endothelial cells

into endothelial cells before keratocytes. On the twentieth day of gestation, the corneal endothelium comprises two cell layers. On day 23, it transforms into a single layer of flattened cells. These results appear in human embryos at 48 days gestation and 8 weeks, respectively (Quantock & Young, 2008). The cellularity of the corneal endothelium decreases during the prenatal period. The decrease in cellularity is attributable to rapid corneal growth and not cell death (Murphy et al., 1984). In agreement with Sevel and Isaacs (1988), the corneal endothelium matures before the corneal epithelium, forming a single cell layer that remains stable throughout embryological development while corneal epithelium, stratification, and maturation occur postnatally.

Examination of electron micrographs revealed that the developing corneal endothelium is composed of highly active cells. They have large euchromatic nuclei and abundant organelles in the cytoplasm. Similar outcomes are documented by (Wulle, 1972). Distended RER in the endothelium indicates active extracellular protein synthesis, and the profusion of organelles is responsible for fibril deposition at the cell's basal side and incorporation into DM (Cintron et al., 1988). Numerous tiny cytoplasmic vesicles were observed in the cellular apices. This replicated the findings of Kaye and Pappas (1962) in rabbits, who determined that pinocytosis is required for transport across the

endothelium due to the presence of terminal bars at the apical ends of the intercellular space between endothelial cells, which can inhibit free diffusion. The endothelial cells also had a solitary cilium. The cilia play no role in fluid transport but serve as receptors (Renard et al., 1976). The development of endothelial cells into regular hexagons and the maintenance of endothelial integrity may depend on these cilia. Changes in the structure and function of the cilia result in aberrant corneal endothelial cell morphology (Song & Zhou, 2020). We observed spaces between the endothelial cells exposing the underlying Descemet's membrane. However, these gaps decrease 2 weeks after birth. When the cornea begins to deturgesce, the spaces between the endothelial cells decrease, according to Cintron et al. (1988).

For achieving and maintaining corneal transparency, corneal avascularity and alymphaticity must be preserved (Chang et al., 2001). In addition to its involvement in corneal neovascularization after injury by increasing microvascular permeability and endothelial fenestration, native VEGF expression in the corneal epithelium regulates corneal wound healing via immunomodulation (Roberts & Palade, 1995). VEGF promotes angiogenesis, preserves epithelial-stromal hemostasis, and controls the stromal fibroblast network and corneal integrity (Wong et al., 2021). Although corneal epithelial cells express VEGF in
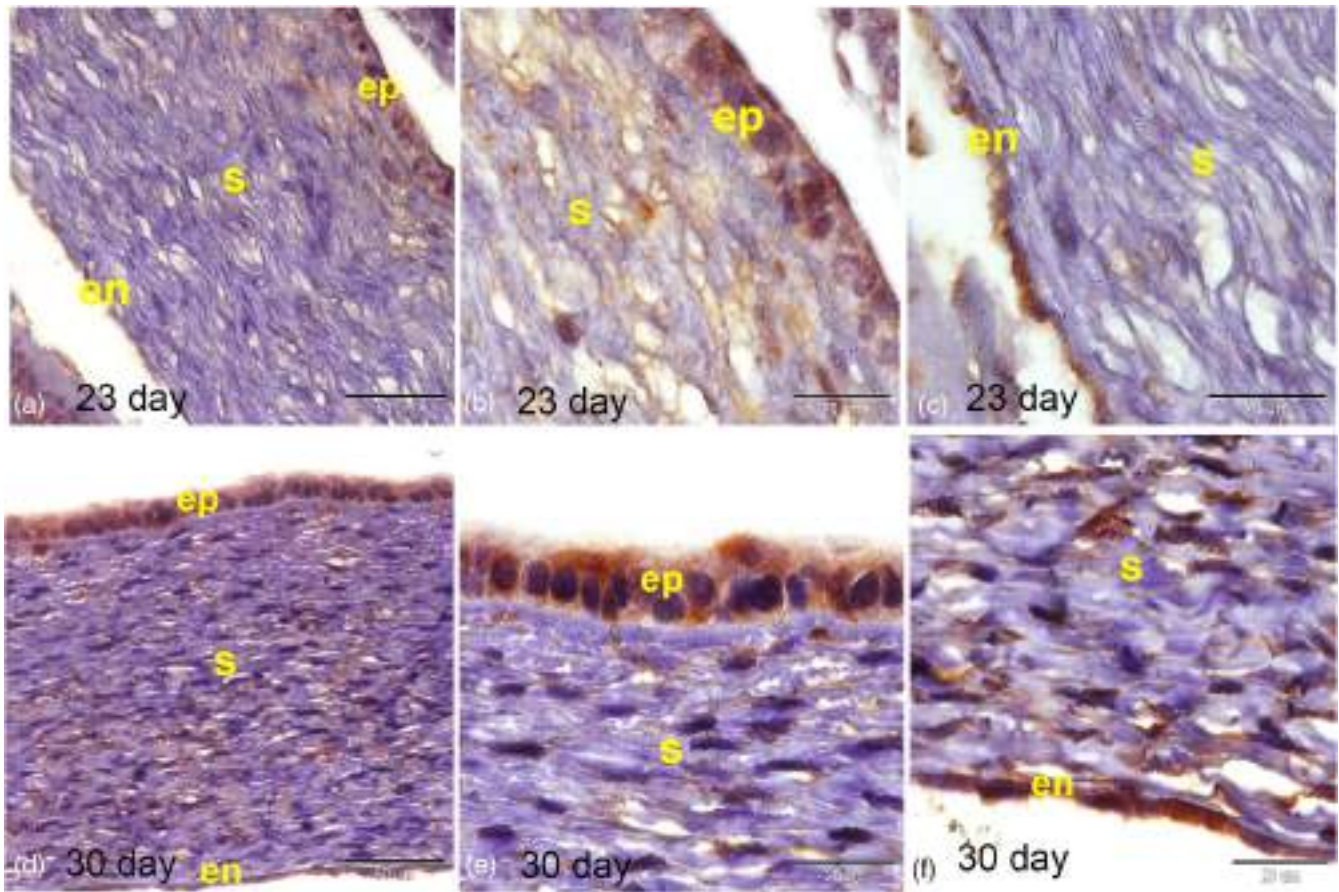
FIGURE 13 VEGF immunostained sections of the developing rabbit cornea prenatally. (a–c) On the 23rd gestational day showing moderate expression of VEGF in the corneal epithelium (ep) and endothelium (en) and mild expression in the stroma (s). (d–f) On the 30th gestational day showing stronger expression of VEGF in the corneal epithelium, stroma and endothelium
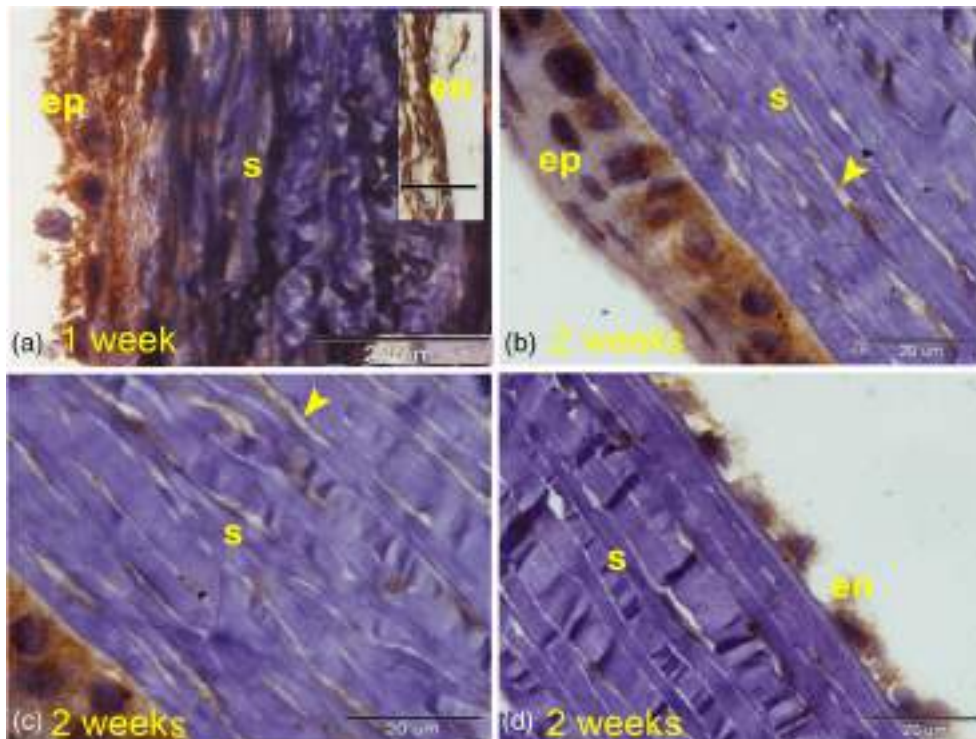

FIGURE 14 VEGF immunostained sections of the developing rabbit cornea postnatally. (a) By the end of the first week after birth showing the intensity of VEGF immunoreactive signals reaches its maximum level in the corneal epithelium (ep), stroma (s) and endothelium (en). (b–d) On the second week after birth showing decreased immunohistochemical localization of VEGF in the rabbit cornea. Take note of the negative immunostaining of the corneal stroma and mild expression of VEGF (arrowheads) in the keratocytes

a normal cornea, potent antiangiogenic factors may neutralize the angiogenic effect of VEGF and keep the cornea avascular (Ma DH et al., 1999). Thus, the balance of angiogenic and antiangiogenic factors maintains corneal avascularity (Cursiefen & Schonherr, 1997; Risau, 1997). In this study, VEGF was expressed by corneal epithelium, stroma, and endothelium. Similar findings were described by van Setten (1997), who detected VEGF expression in the epithelium of the normal cornea, whereas Bednarz et al. (1995) detected the corresponding gene. The current study revealed that the expression of VEGF in the rabbit cornea increases with age and reaches its peak by the end of the first week after birth after which, it decreases in all layers of the cornea, that time of eye lids opening, when the cornea must be avascular and transparent. Interestingly, at this stage, the corneal stroma is immunostained negatively for VEGF, indicating that it has become avascular. However, the keratocytes within the corneal stroma displayed weak VEGF immunostaining. Wong et al. (2021) stated that a well-regulated VEGF expression in keratocytes influences cell arrangement and visual acuity. In addition, they noted that as age increases, VEGF expression decreases, suggesting that the loss of such a receptor leads to a disorganized stromal network and, consequently, poor vision in the elderly.

In conclusion, due to the importance of the cornea for vision, the eyelids do not open until the cornea is fully developed. The cornea must be transparent for maturity. High organization of the lamellae of collagenous fibers and the presence of telocytes within the stroma, which play a role in lamellae arrangement, contribute to corneal transparency. Moreover, the stroma must be devoid of blood vessels. If any factor is compromised, the cornea will lose its transparency and become inoperable.

AUTHOR CONTRIBUTIONS

Research sampling and processing: Nagwa Ibrahim and Sara El-Desoky. Data analysis and interpretation: all authors. Drafting of the manuscript: Nagwa Ibrahim. Critical revision of the manuscript: Wafaa Gaber

CONFLICT OF INTEREST

The authors declare no conflict of interest.

DATA AVAILABILITY STATEMENT

The data that support the findings of this study are available on request from the corresponding author. The data are not publicly available due to privacy or ethical restrictions.

ORCID

Ruwaida Elhanbaly https://orcid.org/0000-0001-7231-2984
Sara M. M. El-Desoky https://orcid.org/0000-0002-8552-9346
Wafaa Gaber https://orcid.org/0000-0003-1754-8489

REFERENCES

Abd-Elhafeez, H. H., & Soliman, S. A. (2017). New description of telocyte sheaths in the bovine uterine tube: An immunohistochemical and scanning microscopic study. *Cells, Tissues, Organs*, *203*, 295–315.

Abd-Elkareem, M. (2017). Cell-specific immuno-localization of progesterone receptor alpha in the rabbit ovary during pregnancy and after parturition. *Animal Reproduction Science*, *180*, 100–120.

Abdel-Maksoud, F. M., Abd-Elhafeez, H. H., & Soliman, S. A. (2019). Morphological changes of telocytes in camel efferent ductules in response to seasonal variations during the reproductive cycle. *Scientific Reports*, *9*, 1–17.

Abdo, M., Haddad, S., & Emam, M. (2017). Development of the *New Zealand* white rabbit eye: I. pre-and postnatal development of eye tunics. *Anatomia, Histologia, Embryologia*, *46*, 423–430.

Albulescu, R., Tanase, C., Codrici, E., Popescu, D. I., Cretoiu, S. M., & Popescu, L. M. (2015). The secretome of myocardial telocytes modulates the activity of cardiac stem cells. *Journal of Cellular and Molecular Medicine*, *19*, 1783–1794.

Al-Taey, O. Y. Y., & Al-Haaik, A. G. (2022). Histomorphometrical and histochemical postnatal development of cornea in indigenous rabbits. *Iraqi Journal of Veterinary Sciences*, *36*, 291–296.

Arey, L. (1965). *Developmental anatomy. A textbook and laboratory manual of embryology* (7th ed.). W. B. Saunders Co.

Bancroft, J. D., Layton, C., & Suvarna, S. K. (2013). *Bancroft 's theory and practice of histological techniques* (7th ed.). Elsevier/Churchill Livingstone.

Bard, J., Bansal, M., & Ross, A. (1988). The extracellular matrix of the developing cornea: Diversity, deposition and function. *Development*, *103*, 195–205.

Bednarz, J., Weich, H. A., Rodokanaki-von Schrenck, A., & Engelmann, K. (1995). Expression of genes coding growth factors and growth factor receptors in differentiated and dedifferentiated human corneal endothelial cells. *Cornea*, *14*, 372–381.

Castro-Combs, J., Noguera, G., Cano, M., Yew, M., Gehlbach, P. L., Palmer, J., & Behrens, A. (2008). Corneal wound healing is modulated by topical application of amniotic fluid in an ex vivo organ culture model. *Experimental Eye Research*, *87*, 56–63.

Chang, J.-H., Gabison, E. E., Kato, T., & Azar, D. T. (2001). Corneal neovascularization. *Current Opinion in Ophthalmology*, *12*, 242–249.

Cintron, C., Covington, H., & Kublin, C. L. (1983). Morphogenesis of rabbit corneal stroma. *Investigative Ophthalmology & Visual Science*, *24*, 543–556.

Cintron, C., Covington, H. I., & Kublin, C. L. (1988). Morphogenesis of rabbit corneal endothelium. *Current Eye Research*, *7*, 913–929.

Cretoiu, D., Xu, J., Xiao, J., & Cretoiu, S. M. (2016). Telocytes and their extracellular vesicles—Evidence and hypotheses. *International Journal of Molecular Sciences*, *17*, 1322.

Cursiefen, C., & Schonherr, U. (1997). Angiogenesis and inhibition of angiogenesis in the eye. *Klinische Monatsblätter für Augenheilkunde*, *210*, 341–351.

Edelstein, L., & Smythies, J. (2014). The role of telocytes in morphogenetic bioelectrical signaling: Once more unto the breach. *Frontiers Media SA*, *7*, 1–3.

El-Desoky, S. M., & Abdellah, N. (2022). The morphogenesis of the rabbit meibomian gland in relation to sex hormones: Immunohistochemical and transmission electron microscopy studies. *BMC Zoology*, *7*, 1–12.

Foster, A., & Gilbert, C. (1992). Epidemiology of childhood blindness. *Eye*, *6*, 173–176.

Graw, J. (2003). The genetic and molecular basis of congenital eye defects. *Nature Reviews Genetics*, 4, 876–888.

Gwon, A. (2008). The rabbit in cataract/IOL surgery. In *Animal models in eye research* (pp. 184–204). Elsevier.

Harper, J. Y., Samuelson, D. A., & Reep, R. L. (2005). Corneal vascularization in the Florida manatee (Trichechus manatus latirostris) and three-dimensional reconstruction of vessels. *Veterinary Ophthalmology*, 8, 89–99.

Hassell, J. R., & Birk, D. E. (2010). The molecular basis of corneal transparency. *Experimental Eye Research*, 91, 326–335.

Haustein, J. (1983). On the ultrastructure of the developing and adult mouse corneal stroma. *Anatomy and Embryology*, 168, 291–305.

Hay, E. D. (1980). Development of the vertebrate cornea. *International Review of Cytology*, 63, 263–322.

Hayashi, S., Osawa, T., & Tohyama, K. (2002). Comparative observations on corneas, with special reference to Bowman's layer and Descemet's membrane in mammals and amphibians. *Journal of Morphology*, 254, 247–258.

Hazlett, L., Spann, B., Wells, P., & Berk, R. (1980). Desquamation of the corneal epithelium in the immature mouse: A scanning and transmission microscopy study. *Experimental Eye Research*, 31, 21–30.

Higazy, M. A. E. M., Selim, K. M., Elsheikh, E. A., & Ismaeel, A. S. (2020). Histopathological changes of the anterior surface structures of rabbit eye after subconjunctival injection of different doses of Mitomycin C. *Al-Azhar International Medical Journal*, 1, 87–96.

Hoffmann, F. (1972). The surface of epithelial cells of the cornea under the scanning electron microscope. *Ophthalmic Research*, 3, 207–214.

Hogan, M. J., ALvarado, J. A., & Wedell, J. E. (1971). *Histology of the human eye*. W.B Saunders Co.

Hussein, M. M., & Mokhtar, D. M. (2018). The roles of telocytes in lung development and angiogenesis: An immunohistochemical, ultrastructural, scanning electron microscopy and morphometrical study. *Developmental Biology*, 443, 137–152.

Jakobiec, F., & Ozanics, V. (1982). General topographic anatomy of the eye. In *Ocular anatomy, embryology, teratology* (pp. 1–9). Harper & Row.

Karnovsky, M. J. (1965). A Formaldehyde glutaraldehyde fixative of high osmolality for use in electron microscopy. *Journal of Cell Biology*, 27, 137A.

Kaye, G. I., & Pappas, G. D. (1962). Studies on the cornea: I. the fine structure of the rabbit cornea and the uptake and transport of colloidal particles by the cornea in vivo. *The Journal of Cell Biology*, 12, 457–479.

Kurata, M., Yamagiwa, Y., Haranosono, Y., & Sakaki, H. (2017). Repeated-dose ocular instillation toxicity study: A survey of its study design on the basis of common technical documents in Japan. *Fundamental Toxicological Sciences*, 4, 95–99.

Lovicu, F. J., Kao, W. W.-Y., & Overbeek, P. A. (1999). Ectopic gland induction by lens-specific expression of keratinocyte growth factor (FGF-7) in transgenic mice. *Mechanisms of Development*, 88, 43–53.

Luesma, M. J., Gherghiceanu, M., & Popescu, L. M. (2013). Telocytes and stem cells in limbus and uvea of mouse eye. *Journal of Cellular and Molecular Medicine*, 17, 1016–1024.

Ma, D. H. K., Tsai, R. J. F., Chu, W. K., Kao, C. H., & Chen, J. K. (1999). Inhibition of vascular endothelial cell morphogenesis in cultures by limbal epithelial cells. *Investigative Ophthalmology and Visual Science*, 40, 1822–1828.

Marini, M., Mencucci, R., Rosa, I., Favuzza, E., Guasti, D., Ibba-Manneschi, L., & Manetti, M. (2017). Telocytes in normal and keratoconic human cornea: An immunohistochemical and transmission electron microscopy study. *Journal of Cellular and Molecular Medicine*, 21, 3602–3611.

Maurice, D. M. (1985). *The cornea and the sclera*. Academic Press.

Merindano, M. D., Costa, J., Canals, M., Potau, J., & Ruano, D. (2003). A comparative study of Bowman's layer in some mammals: Relationships with other constituent corneal structures. *European Journal of Anatomy*, 6, 133–140.

Murphy, C., Alvarado, J., Juster, R., & Maglio, M. (1984). Prenatal and postnatal cellularity of the human corneal endothelium. A quantitative histologic study. *Investigative Ophthalmology and Visual Science*, 25, 312–322.

Pei, Y., & Rhodin, J. (1970). The prenatal development of the mouse eye. *The Anatomical Record*, 168, 105–125.

Pfister, R. R. (1973). The normal surface of corneal epithelium: A scanning electron microscopic study. *Investigative Ophthalmology and Visual Science*, 12, 654–668.

Pinnock, A., Shivshetty, N., Roy, S., Rimmer, S., Douglas, I., MacNeil, S., & Garg, P. (2017). Ex vivo rabbit and human corneas as models for bacterial and fungal keratitis. *Graefe's Archive for Clinical and Experimental Ophthalmology*, 255, 333–342.

Quantock, A. J., & Young, R. D. (2008). Development of the corneal stroma, and the collagen–proteoglycan associations that help define its structure and function. *Developmental Dynamic*, 237, 2607–2621.

Renard, G., Hirsch, M., Galle, P., & Pouliquen, Y. (1976). Ciliated cells of corneal endothelium. Functional and morphological aspects compared to cilia of other organs. *Archives D'ophtalmologie*, 36, 59–72.

Reynolds, E. S. (1963). The use of lead citrate at high pH as an electron-opaque stain in electron microscopy. *The Journal of Cell Biology*, 17, 208–212.

Risau, W. (1997). Mechanisms of angiogenesis. *Nature*, 386, 671–674.

Roberts, W. G., & Palade, G. E. (1995). Increased microvascular permeability and endothelial fenestration induced by vascular endothelial growth factor. *Journal of Cell Science*, 108, 2369–2379.

Robinson, G. C., Jan, J. E., & Kinnis, C. (1987). Congenital ocular blindness in children, 1945 to 1984. *American Journal of Diseases of Children*, 141, 1321–1324.

Saika, S., Saika, S., Liu, C.-Y., Azhar, M., Sanford, L. P., Doetschman, T., Gendron, R. L., Kao, C. W.-C., & Kao, W. W.-Y. (2001). TGFβ2 in corneal morphogenesis during mouse embryonic development. *Developmental Biology*, 240, 419–432.

Sevel, D., & Isaacs, R. (1988). A re-evaluation of corneal development. *Transactions of the American Ophthalmological Society*, 86, 178–207.

Song, T., & Zhou, J. (2020). Primary cilia in corneal development and disease. *Zoological Research*, 41, 1–8.

Swamynathan, S. K. (2013). Ocular surface development and gene expression. *Journal of Ophthalmology*, 2013, 1–22.

Tang, L., Song, D., Qi, R., Zhu, B., & Wang, X. (2022). Roles of pulmonary telocytes in airway epithelia to benefit experimental acute lung injury through production of telocyte-driven mediators and exosomes. *Cell Biology and Toxicology*, 38, 1–15.

Van Cruchten, S., Vrolyk, V., Perron Lepage, M. F., Baudon, M., Voute, H., Schoofs, S., Haruna, J., Benoit-Biancamano, M. O., Ruot, B., & Allegaert, K. (2017). Pre-and postnatal development of the eye: A species comparison. *Birth Defects Research*, 109, 1540–1567.

Van Setten, G. B. (1997). Vascular endothelial growth factor (VEGF) in normal human corneal epithelium: Detection and physiological importance. *Acta Ophthalmologica Scandinavica*, 75, 649–652.

Vazirani, J., & Basu, S. (2013). Keratoconus: Current perspectives. *Clinical Ophthalmology (Auckland, NZ)*, 7, 2019.

Wong, H. L., Poon, S. H. L., Bu, Y., Lo, A. C. Y., Jhanji, V., Chan, Y. K., & Shih, K. C. (2021). A systematic review on cornea epithelial-stromal homeostasis. *Ophthalmic Research*, 64, 178–191.

Wulle, K. G. (1972). Electron microscopy of the fetal development of the corneal endothelium and Descemet's membrane of the human eye. *Investigative Ophthalmology and Visual Science*, *11*, 897–904.

Yamagiwa, Y., Kurata, M., & Satoh, H. (2021). Histological features of post-natal development of the eye in white rabbits. *Toxicologic Pathology*, *49*, 419–437.

Zhang, Z. Y., Hoffman, M. R., Zhou, X. T., Xu, Y., Zhang, X. R., Chu, R. Y., & Chen, C. D. (2014). Refractive change in the adult rabbit eye after corneal relaxation with the femtosecond laser. *BMC Ophthalmology*, *14*, 1–6.